67-96

MODEL OF AN ELECTRIC ARC BALANCED MAGNETICALLY IN A GAS FLOW

by

ARNOLD M. KUETHE, ROBERT L. HARVEY and LELAND M. NICOLAI
The University of Michigan
Ann Arbor, Michigan

AIAA Paper
No. 67-96

AIAA
5th Aerospace Sciences Meeting
NEW YORK, NEW YORK / JANUARY 23-26, 1967

MODEL OF AN ELECTRIC ARC BALANCED MAGNETICALLY IN A GAS FLOW*

Arnold M. Kuethe, Robert L. Harvey,
and Leland M. Nicolai
The University of Michigan
Ann Arbor, Michigan

1. INTRODUCTION

A persistent question relative to a convected or balanced arc has been that of determining whether the arc simulates a solid cylinder or whether the phenomenon is a "flow-through" process. In this paper a fluid mechanical model of the arc is developed on the basis of photographs which show that the arc must simulate a solid body.

The experimental data were obtained on the equipment developed by Bond,[1] and on which he showed for the first time that an arc could be balanced magnetically in a high speed airstream and that the arc is stable in a supersonic flow if it can assume a characteristic slant angle near the Mach angle of the incident flow.[2,3] Other significant properties of the balanced arc are also given in these references. Figure 1 demonstrates the relative orientation of the velocity, magnetic, and electric fields for the balanced arc. The intensity of the external magnetic field was around 20 times that of the self-field.

In the following sections evidence is given that, with some qualifications, (1) the balanced arc can be treated as a steady phenomenon, (2) the dynamics of the arc plasma in a uniform magnetic field can be treated by the equations of continuum fluid mechanics, (3) the arc simulates approximately an infinite solid cylinder of uniform cross section, (4) the internal flow and a boundary layer flow can be treated separately. The dimensionless parameters, the governing equations and the boundary conditions are discussed and the equations simplified for the inner and outer flows.

2. ARC AS A STEADY PHENOMENON

High speed motion pictures by Bond[1] showed for the first time that an arc can be balanced magnetically as well as stabilized in a high speed cross flow.

*Supported by NASA Grant NGR 23-006-128

The arc was balanced magnetically between rails parallel to a supersonic flow; the photographs showed the arc to be remarkably steady if the streamwise location of the force balance (Fig. 1) permitted the arc to assume a characteristic slant angle. The slant angle was found to be near the Mach angle, which is also the angle for maximum degree of ionization within the arc.

3. THE ARC AS AN IMPERVIOUS BODY

An axial flow along the arc, which is a sufficient condition that the exterior stream flows around rather than through the arc, was observed by the first two authors.[4] High speed motion pictures taken in the setup described in reference 1 show small masses of vaporizing copper moving along the arc from anode to cathode; one such sequence is shown in Fig. 2.

The vaporizing particle moves along the arc at about 35 ft/sec, while the speed of the free stream is about 1800 ft/sec. The proof that the arc simulates a solid cylinder lies in the fact that if the flow were through, rather than around, the arc the vaporizing particle would be swept downstream long before it could reach the cathode.

The measured speed of the particle along the arc is a lower bound of the axial flow because of the weight of the vaporizing particles being photographed; the cathode is above the anode so the gravitational force retards the upward motion of the particles. In one run a particle actually remains stationary within the arc for several frames indicating that its weight was equal to the drag exerted on it by the axial flow. Experiments utilizing injected gases instead of solid particles are under preparation.

The tracer studies were made in the slanted arc at Mach numbers 2.5 and 3.5. Roman[5] has since, on the basis of photographs and flow measurements confirmed the solid cylinder simulation for a balanced arc in a subsonic free jet.

4. GENERAL EQUATIONS

In what follows the arc is approximated by a cylinder of constant cross-section so that the flow, both internal and external, may be treated as two-dimensional relative to coordinates in the plane normal to the axis of the arc. The approximation will be far from reality near the roots but it is expected to give satisfactory results at stations midway between the arc roots, particularly if the ratio of the arc length to the major dimension is large.

Estimates (see section 5) indicate that the average arc temperatures over the range of operating conditions in air are around 7000°K. We may therefore treat the arc plasma as weakly ionized. Also, radiation effects are neglected and we approximate the conservation equations by those for a perfect gas:

$$\rho(\vec{V}\cdot\nabla)\vec{V} = -\nabla P + \vec{J}\times\vec{B} + \nabla(\mu\nabla\cdot\vec{V}) \tag{1}$$

$$\rho c_p\vec{V}\cdot\nabla T = \vec{V}\cdot\nabla P + \nabla\cdot(k\nabla T) + \vec{E}\cdot\vec{J} + \Phi \tag{2}$$

$$\nabla\cdot(\rho V) = \epsilon(x,y) \tag{3}$$

ρ, $\vec{V}$, P, μ, k, T, Φ are, respectively, the fluid density, velocity, pressure, viscosity, heat conduction, temperature, and rate of viscous dissipation; $\vec{J}$ is the current density, $\vec{B}$ the magnetic induction, $\vec{E}$ the electric field, ϵ the source strength (mass drawn per second from the axial flow to make up for the rate of transfer to the free stream at the boundary).

Since the external magnetic field is around 20 times that of the self-field the magnetic induction $\vec{B}$ is taken as constant and equal to that for the external field. The plasma velocity will be small and if we neglect Hall currents,

$$\left.\begin{aligned} \vec{J} &= \sigma\vec{E} = J(T) \\ \vec{E}\cdot\vec{J} &= EJ \end{aligned}\right\} \tag{4}$$

In the experimental setup used, the airflow is in the x direction, $\vec{B} = B\vec{e}_y$, where $\vec{e}_y$ is the unit vector in the y direction, and $\vec{J} = J\vec{e}_z$. Then

$$\vec{J}\times\vec{B} = -JB\,\vec{e}_x \tag{5}$$

In succeeding sections these equations will be particularized for the internal and external flows.

5. GENERAL PROPERTIES OF INTERNAL FLOW

Equations (1)-(5) describe a circulation generated by a variable Lorentz force $-JB\vec{e}_x$ acting upstream on an element of plasma within the balanced arc; the phenomenon is conceptually analogous to the generation of convection currents by gravity forces acting on a gas within a horizontal cylindrical tube which is heated over the central region. The electric current density within the arc is in general a maximum at the center; then an element with current density greater than that required by the balance between Lorentz and pressure force will be accelerated toward the upstream boundary. Schematic streamlines are shown in Fig. 3. We show in section 6 that EJ, the joule heating term in Eq. (2), is much larger than the diffusion term in the interior of the arc so that the temperature of the element and, therefore, the electric current density increase while the element moves toward the upstream boundary; in the vicinity of the arc boundary the pressure gradient generated in the external flow deflects the element in the streamwise direction along the boundary. At some point near the boundary the diffusion term in Eq. (2) will dominate and the elements in the vicinity will suffer a decrease in temperature, density, and Lorentz force. They will accordingly be accelerated sufficiently by the pressure gradient so they enter the wake and are swept downstream.

The streamlines shown in Fig. 3 are schematically the projections of the paths of fluid elements on the arc cross section. The rate of mass transfer to the external flow at a given station along the arc is, under steady conditions, equal to the source strength at that station (see Eq. (3)). It is clear that the mass lost at the boundary must be only a small part of the axial mass flow; otherwise there would be serious departures from effective two-dimensionality of the internal flow.

As a result of the internal circulation, the plasma properties will tend toward uniformity over the cross-section. It follows that the more intense the circulation the greater will be the tendency toward uniformity over a core and, hence, toward the formation of a "boundary layer" at the arc boundary within which large gradients in momentum, temperature and density exist.

The arc boundary will be determined by the condition that at each point the fluid pressure outside must equal the magnetic pressure inside (the fluid pressure inside may be neglected because of the low density and relatively low internal velocities). The boundary shape thus determined will depend on the incident velocity, density, and pressure, on the electric current and current density, on the external and self magnetic fields, on flow interference caused by other bodies in the flow, stream boundaries, etc.

The above flow can be expressed in terms of the conservation equations in forms analogous to those used to describe heat convection. The following non-dimensional parameters are defined:

$$\left.\begin{array}{l} j = \dfrac{J}{J_1}, \quad \vec{u} = \dfrac{V}{U_1}, \quad p = \dfrac{P}{\rho U_1^2}, \quad x = \dfrac{X}{d}, \quad y = \dfrac{Y}{d} \\ \tau = \dfrac{U_1 t}{d}, \quad \Theta = \dfrac{T}{T_1}, \quad Re_1 = \dfrac{\bar{\rho} U_1 d}{\bar{\mu}}, \quad Gr_m = \dfrac{\bar{\rho} J_1 B d^3}{\bar{\mu}^2} \\ Pr_1 = \dfrac{c_p \bar{\mu}}{k}, \quad K_1 = \dfrac{U_1^2}{c_p T_1}, \quad S = \dfrac{E J_1 d}{\bar{\rho} c_p T_1 U_1} \end{array}\right\} \tag{6}$$

After replacing ρ and μ by their average values, $\bar{\rho}$ and $\bar{\mu}$, Eqs. (1)-(3) with (4) and (5) become

$$\frac{d\vec{u}}{d\tau} = - \text{grad } p - \frac{Gr_m}{Re_1^2} j \vec{e}_x + \frac{1}{Re_1} \nabla^2 \vec{u} \tag{7}$$

$$\frac{d\Theta}{d\tau} = K_1 \frac{dp}{d\tau} - \frac{1}{Pr_1 Re_1} \nabla^2 \Theta + Sj + \frac{K_1}{Re_1} \Phi \tag{8}$$

$$\text{div } \vec{u} = \frac{\varepsilon d}{U_1 \bar{\rho}} \tag{9}$$

where d is a characteristic length and U_1, T_1, and J_1 are, respectively, characteristic velocity, temperature, and current density.

In addition to the Reynolds, Prandtl, and Eckert numbers, respectively Re_1, Pr_1, and K_1, the following parameters are significant in determining the physical aspects of the internal flow.

The role of the modified Grashof number Gr_m in determining the intensity of the circulation within the arc is roughly analogous to that of the conventional Grashof number $Gr = \beta g \Delta\Theta d^3/\nu^2$ (β is the expansion coefficient of the fluid, g is the acceleration of gravity, and $\Delta\Theta = \Delta T/T_1$) in determining the intensity of the circulation of a gas within a horizontal cylinder with nonuniform temperature distribution over the cross-section. We see that in the modified Grashof number the Lorentz acceleration $jB/\bar{\rho}$ replaces the gravitational acceleration $\beta g \Delta\Theta$. Reference to Eq. (7) shows that the ratio of the Lorentz to the viscous force on a representative element is Gr_m/Re_1, and the Lorentz to the inertia force is Gr_m/Re_1^2. In the analysis given here we write $J_1 d^2 = I$, so that

$$Gr_m = \frac{\bar{\rho} I B d}{\bar{\mu}^2} \tag{10}$$

A satisfactory qualitative analogy between the circulation within a balanced arc and that in a horizontal heated cylinder of gas is to be expected, even though the joule heating term EJ (or Sj in Eq. (8)) has no counterpart in the convection problem. In fact, the effect of this term would be to increase the velocity of a plasma element because as it is heated the current density and therefore the Lorentz force increase.

The characteristic velocity for the internal flow is not known; we therefore choose the counterpart of that defined by Ostrach in the heat convection problem, that is,

$$U_1 = \sqrt{(J_1 B/\overline{\rho})d} \qquad (11)$$

so that

$$Re_1 = \sqrt{Gr_m} \qquad (12)$$

Equation (11) represents an upper bound for the internal velocity, provided the circulation within the arc does not depend directly on the external flow. By use of Eq. (12), Eq. (7) may be written

$$\frac{d\vec{u}}{dt} = - \text{grad } p - j\vec{e}_x + \frac{1}{\sqrt{Gr_m}} \nabla^2\vec{u} \qquad (13)$$

For high Grashof numbers Eq. (13) is of the boundary layer type, since the coefficient of the highest order term is small. Under these circumstances, then, the arc will consist of an inner core of relatively uniform properties and a thin boundary layer within which the properties change through high gradients from their core values to those in the free stream.

Some indication of the extent to which transfer from the arc to the external stream takes place through a thin boundary layer can be gained by comparing the calculated heat transfer from a solid cylinder at the same mean temperature as the arc with the joule heating within the steady arc. Figure 4 is a plot of Q/EI versus $\sqrt{Gr_m}$ for observations at Mach numbers 2.5 and 3.5; Q is the calculated rate of heat transfer from a solid cylinder[7,8,9] at the same temperature and with surface area equal to that indicated for the arc by two simultaneous photographs taken along lines about 90° to each other; EI is the rate of joule heating of the arc; in Eq. (10) for Gr_m, $\overline{\rho}$ and $\overline{\mu}$ are taken as the mean values over the arc, and d is the arc width normal to the flow. The mean temperature of the arc was approximated from the indicated cross-sectional area, and the measured total current and electric field. Mean temperatures so calculated varied between about 6000° and 8000°K. The values of Q/EI show some dependence on Mach number which may stem from imperfection in the analogy between the slanted arc and a slanted solid cylinder of uniform cross-section or from the general applicability of the assumption expressed by Eq. (11). However, the trend of the ratio with Grashof number is reasonable on the basis that, as the Grashof number increases the circulation within the arc will become more intense and also the rate at which heat is transferred to the stream by mass transfer will increase. Therefore, heat is convected to the boundary at a higher rate the higher the Grashof number. The fact that the trend carries the ratio farther from unity is probably not significant, considering the approximate nature of the comparison and the fact that the data that form the basis for the calculations apply to circular cylinders at temperatures much lower than those of the arc.

Then, considering the approximate nature of the comparison, the values of Q/EI is Fig. 4 are remarkably close to unity. Therefore, since heat transfer from the solid cylinder takes place through a thin boundary layer, we conclude that high temperature gradients must exist at the arc boundary as well, and thus that a core of relatively uniform properties obtains.

We may also reason that both temperature and velocity boundary layers must be thin because the coefficients of the highest order terms in Eqs. (7) and (8) are both small; the Prandtl number is not significantly different from unity over the range of temperatures involved.[9]

6 CIRCULATION WITHIN THE CORE

Equations (1)-(3) applied to the core flow may be simplified if we may consider the flow field as generated by a perturbation on a uniform current density. This superposition is justified if the velocities generated are small and if the flow is incompressible, that is, if the Grashof number is high enough so that the perturbations are small enough that we may write

$$J = J_o + J' \qquad (14)$$

such that $-J_o B\vec{e}_x$ is equal everywhere to the pressure gradient required to balance the arc. Then, with

$$\frac{\partial p}{\partial x} = -J_o B\vec{e}_x \qquad (15)$$

Eq. (7), which already postulates incompressible flow, becomes

$$\frac{d\vec{u}}{dt} = -\frac{Gr_m}{Re_1^2} j'\vec{e}_x - \frac{\partial p}{\partial y}\vec{e}_y + \mu\nabla^2\vec{u} \tag{16}$$

where $j = J'/J_o$ and $J_o = J_1$ in Eq. (10). In Eq. (8) the first and last terms on the right vanish, since K is proportional to the square of the Mach number. The characteristic velocity, defined in Eq. (11) for the complete arc, is now defined as the perturbation velocity

$$U_1' = \sqrt{(J'_{max}B/\rho)d} \tag{17}$$

To be consistent T_1 becomes $T_1' = T_{max.} - T_o$ and the ratio of the joule heating rate of a representative element to its heat diffusion rates is (Eq. (8))

$$S\ Pr_1\ Re_1 = \frac{EJ_o d^2}{kT_1'} = \frac{EI}{kT_1'} \tag{18}$$

With k = 2 Btu/hr ft°R at 7000°K,[7] and assuming $T_1' = 100°K$, E = 400 volts/ft, I = 200 amps the above ratio is about 10^3. We therefore may neglect all but the convection and joule heating terms in Eq. (8) applied to the arc core.

The value of U_1 given by Eq. (17) will be small, particularly at high Grashof numbers. Under these circumstances we may neglect the convection terms in Eq. (16) and Eqs. (1)-(3) become in the core region

$$J'B = \mu\nabla^2 u \tag{19}$$

$$\frac{\partial p}{\partial y} = \mu\nabla^2 v \tag{20}$$

$$\frac{d\theta'}{dt} = EJ \tag{21}$$

$$\frac{\partial u}{\partial x} + \frac{\partial v}{\partial y} = \frac{\epsilon}{\rho} \tag{22}$$

The conditions to be met are that the magnetic pressure must equal the fluid pressure at every point on the arc boundary. It would be necessary to postulate a source strength and distribution in Eq. (22) and determine a distribution of J and J' such that a steady flow satisfies the pressure condition at the boundary for one of a family of predetermined cross-section shapes. Extensive machine computation appears inevitable.

7. THE BOUNDARY LAYER

Figure 5 illustrates the physical process by which a momentum boundary layer is established. The pressure gradient in the flow along the surface is opposed by a component of the Lorentz force acting on an element of the plasma at the arc boundary. Thus a momentum gradient develops throughout the layer within which the current density decreases from the value representative of the arc core to substantially zero. The following example indicates that the reduction in momentum at the boundary will be considerable: At Mach 3.5, a stagnation pressure of one atmospheres, an arc current of 300 Amperes, and a magnetic field of 1540 Gauss, the dimensions of the luminous portion of the arc are 0.032 x 0.023 ft; assuming that the electric current density within the luminous portion of the arc is constant, $J = 5.2 \times 10^5$ Amps/ft^2, and the Lorentz force is 5.5×10^3 lbs/ft^3. We now compare this force with the maximum pressure gradient in the plane normal to the slanted arc (Mach number for the velocity component normal to arc is approximately unity) for a circular cylinder of the same area as the arc.[10] This maximum gradient is 6.1×10^3 lbs/ft^3; it occurs at 65° from the stagnation point. Thus the component of the Lorentz force opposing the pressure gradient is about $0.9 \times 5.5 \times 10^3 = 5.0 \times 10^3$ lbs/ft^3. A close comparison of the above numbers is not meaningful but the fact that they are not significantly different indicates that an element of arc plasma at the boundary will be nearly in equilibrium and therefore that the momentum of the plasma at the arc boundary is small compared with that of the free stream.

The ratio between the density in the core and that in the free stream is about 0.01. Thus a small net force on the plasma element would cause high accelerations near the arc boundary. For this reason instead of a velocity boundary layer we must direct our consideration to the momentum layer.

Considering that virtually the entire changes in the properties take place within the boundary layer, simplifications of the conservation equations applicable throughout the layer do not appear feasible. With the ordinary boundary layer approximations Eqs. (1) and (2) become

$$\left.\begin{aligned}
\rho \frac{du_s}{dt} &= -\frac{\partial p}{\partial s} - JB\sin(n,x) + \frac{\partial}{\partial n}\left(\mu \frac{\partial u_s}{\partial n}\right) \\
\rho c_p \frac{dT}{dt} &= u\frac{\partial p}{\partial x} + \frac{\partial}{\partial n}\left(k\frac{\partial T}{\partial n}\right) + EJ + \mu\left(\frac{\partial u_s}{\partial n}\right)^2 \\
\frac{\partial}{\partial s}(\rho u_s) &+ \frac{\partial}{\partial n}(\rho v_s) = 0 \\
J &= J(T,p)
\end{aligned}\right\} \qquad (23)$$

with boundary conditions:

$$\text{at} \quad n = 0 : u_s = u_o \ , \ v_s = v_o \ , \ T = T_o$$

$$\text{at} \quad n = \infty : u_s = u_\infty \ , \quad T = T_\infty$$

The boundary conditions at $n = 0$, as well as the shape of the boundary corresponding to $n = 0$, must be given by the solutions in the core described by the solution of the equations described in section 6.

8. MEASURED PROPERTIES

Measurements of the arc dimensions were made relatively easy by the fact that the arc boundary at least over the upstream portion is quite distinct as shown on high speed motion pictures. This circumstance supports the prediction given here that a thin boundary layer exists through which the transfer takes place.

Figure 6 shows some arc dimensions at Mach 3.5, atmospheric stagnation pressure. The dimensions were measured by means of simultaneous photographs of a head-on view and a view of the arc reflected at the tunnel wall. The ratio of d_f the front view to d_s the side view is about 1.3 over the range of arc currents from 130 to 500 amperes.

The calculated values of current density are based on the assumptions that the luminous portion represents the core of relatively constant properties and that the cross-section as elliptical. The voltage drop along the column was measured at two gaps and varied from 20 to 30 volts per inch. Then the temperature range indicated by these values is from 6200 to 7800°K.

Values of the normal force coefficient versus Reynolds number for the component normal to the arc are shown for two Mach numbers in Fig. 7. The values show considerable variation with Mach number but the values are in the range for solid circular cylinders at Mach numbers around one.[11]

9. CONCLUSIONS

On the basis of high speed motion pictures we conclude that a magnetically balanced steady arc simulates a solid body in a gas flow.

Assuming that the arc simulates a solid cylinder of uniform cross-section with axial flow a two-dimensional model is proposed. The model, applicable at high modified Grashof numbers, comprises an inner core of nearly constant properties, and a boundary layer circulation within the core carries the heat to the edge of the boundary layer, which then transfers it through conduction to the external flow.

REFERENCES

1. Bond, C. E., "Magnetic Confinement of an Electric Arc in Transverse Supersonic Flow," AIAA J., 3, 142 (1965).

2. Bond, C. E., "The Magnetic Stabilization of an Electric Arc in Supersonic Flow," Ph.D. dissertation, The University of Michigan (1964) also ARL 65-185, October, 1965.

3. Bond, C. E , "Slanting of a Magnetically Stabilized Electric Arc in Transverse Supersonic Flow," Phys. Fluids 9, 705 (1963).

4. Progress Report, February 28, 1965, Contract AF33(657)-8819 and Final Report, June 1, 1965, Monitored by Thermomechanics Branch, Aerospace Research Laboratories, Wright-Patterson Air Force Base, Ohio.

5. Roman, W. C., "Investigation of Electric Arc Interaction with Aerodynamic and Magnetic Fields," Ph.D. dissertation, Ohio State University (1965).

6. Ostrach, Simon, Part F, Vol. 4, High Speed Aerodynamics and Jet Propulsion, F. K. Moore, Ed., Princeton University Press, 1964.

7. Jokob, M., Heat Transfer, (John Wiley and Sons, Inc., New York, 1949), Vol. 1, p. 560.

8. John, R., Bade, W., Liebermann, R. W., "Theoretical and Experimental Investigation of Arc Plasma-Generation Technology, Part II, Vol. 2, ASD-TDR-62-729, September, 1963.

9. Ragent, B., Nobel, C. E., "High-Temperature Transport Coefficients of Selected Gases," ARL 62-328, April, 1962.

10. Mair, W. A. and Beavan, J. A., Ch. 12, Modern Developments in Fluid Dynamics—High Speed Flow, L. Howarth, Ed., p. 685, Oxford University Press, 1953.

11. Hoerner, S. F., Fluid-Dynamic Drag, 2nd Edition, Published by Author, 1965.

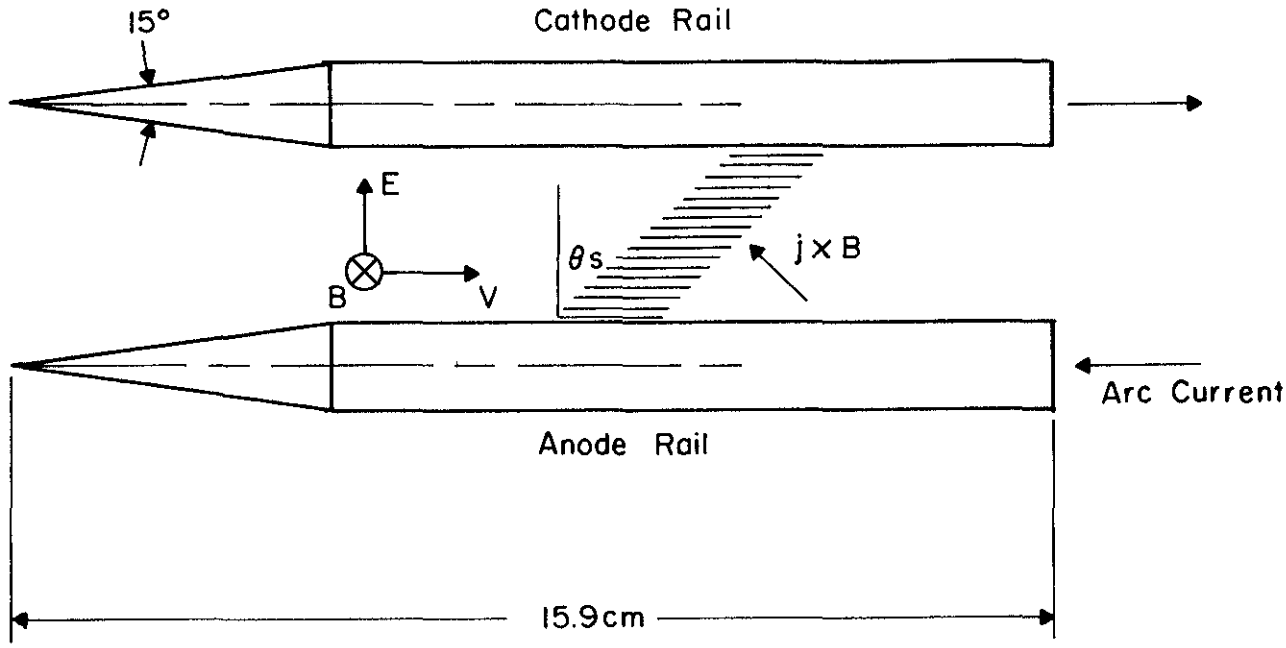

Figure 1. Relative orientation of the velocity, magnetic, and electric fields.

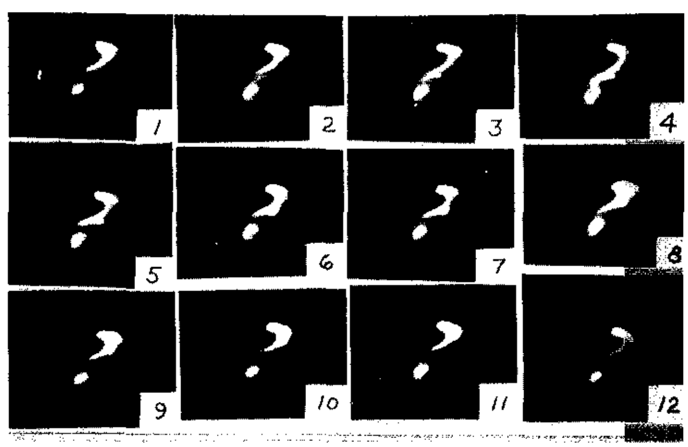

Figure 2. Film sequence showing particle moving from anode to cathode. Mach number 2.5. Film speed about 3000 exposures per second.

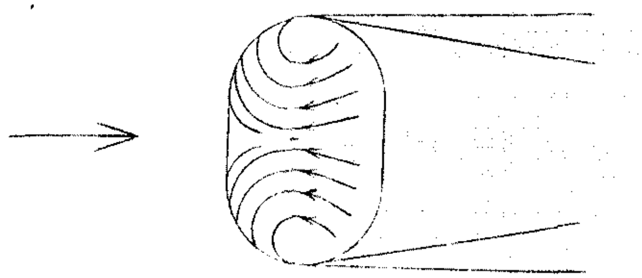

Figure 3. Qualitative model of balanced arc.

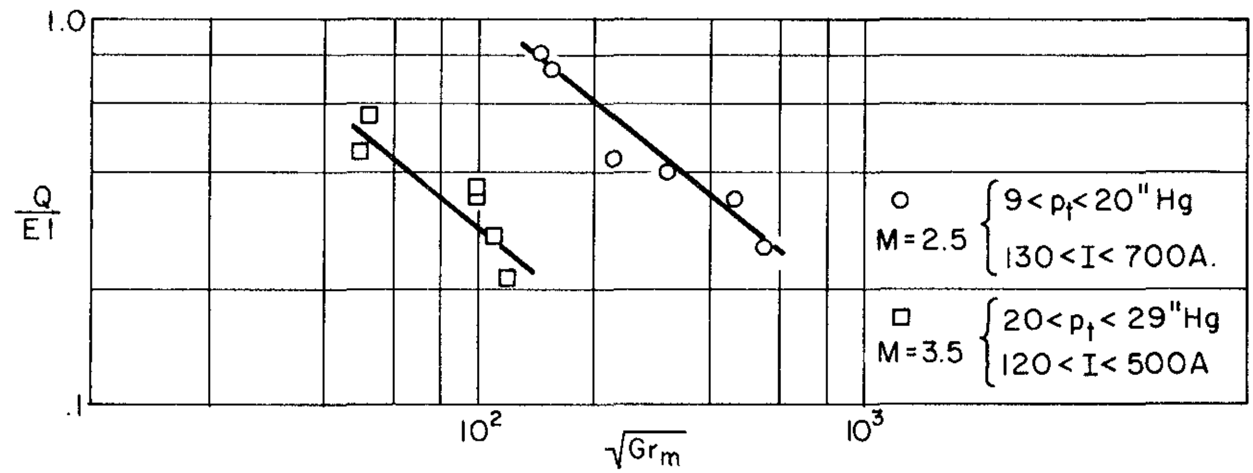

Figure 4.

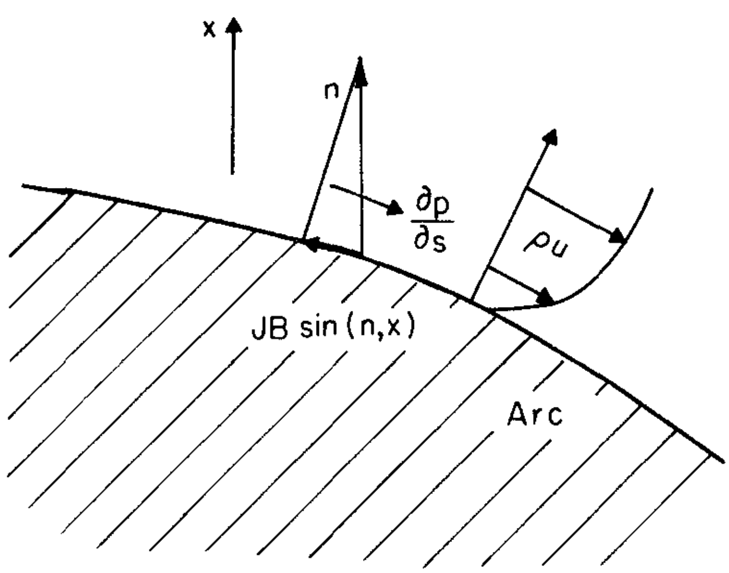

Figure 5. Boundary layer formation.

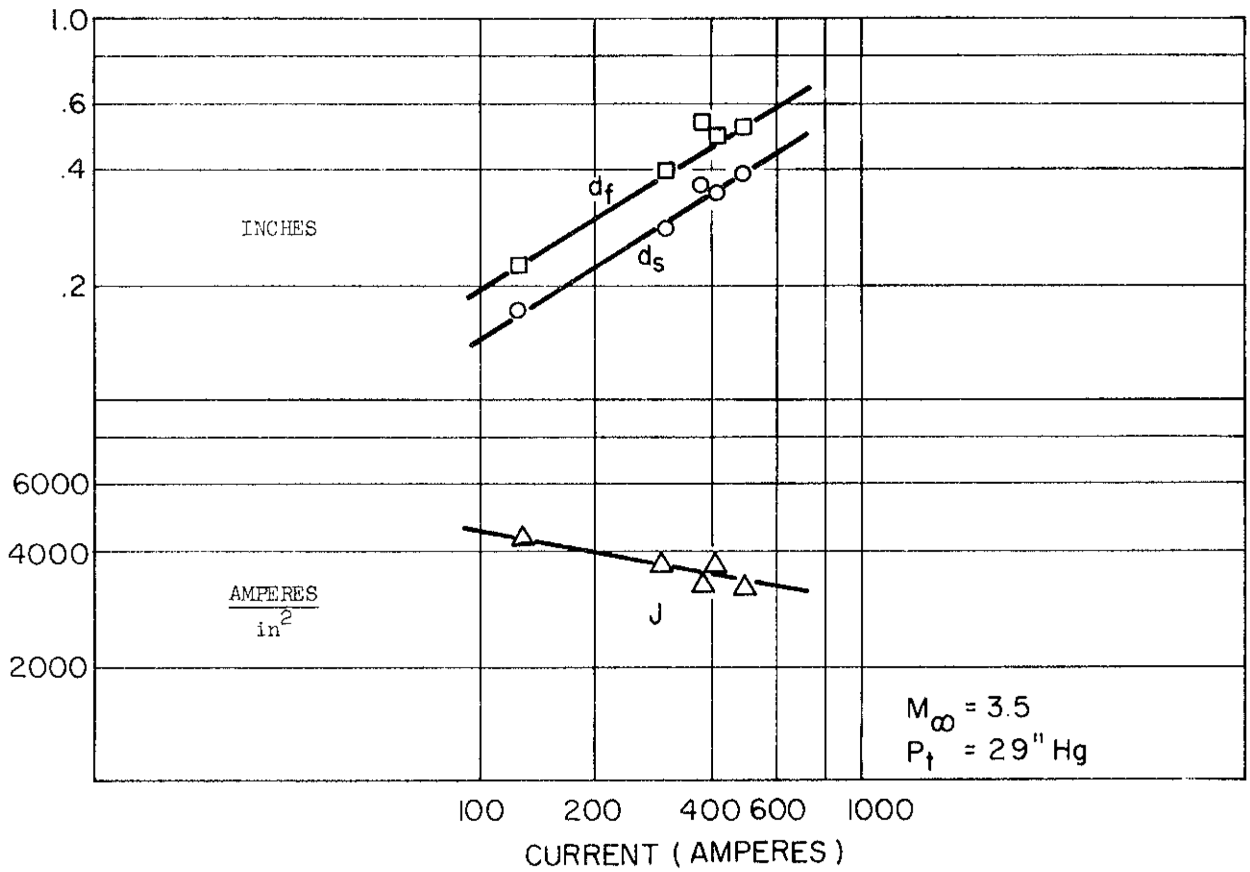

Figure 6. Current density and arc dimensions.

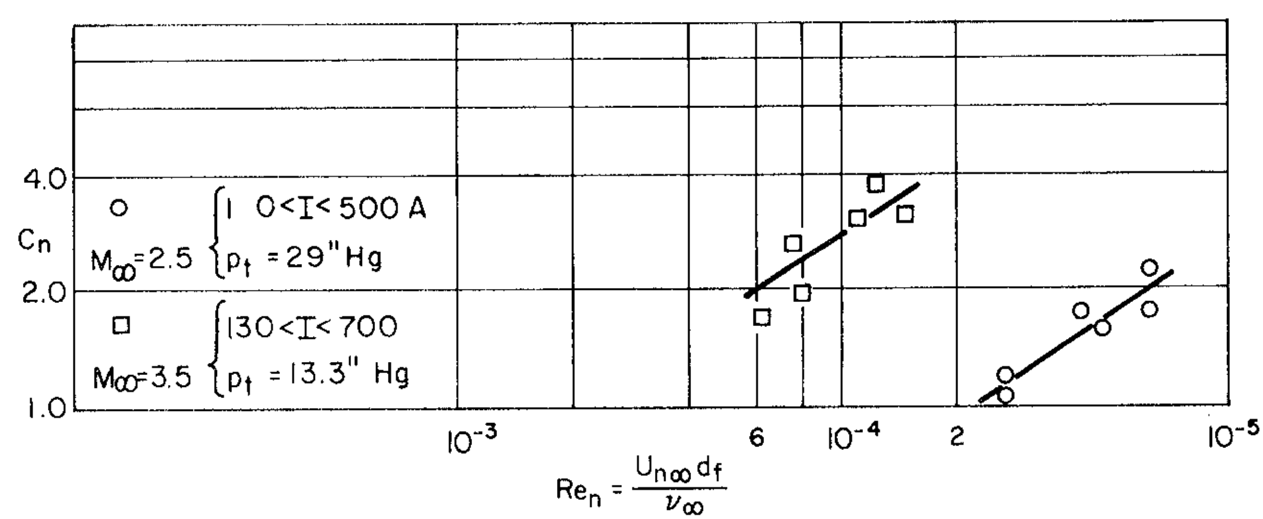

Figure 7. Normal force coefficient referred to the normal velocity component versus the normal Reynolds number based upon free properties.